



Quality-by-Design Approach Development, Characterization, and In Vitro Release Mechanism Elucidation of Nanostructured Lipid Carriers for Quetiapine Fumarate Oral Delivery

Olfa Ben Hadj Ayed¹ · Mohamed Ali Lassoued¹ · Souad Sfar¹

Accepted: 3 June 2021 / Published online: 16 June 2021

© The Author(s), under exclusive licence to Springer Science+Business Media, LLC, part of Springer Nature 2021

Abstract

Purpose The objective of this work was to develop a new nanostructured lipid carrier (NLC) formulation for the oral delivery of quetiapine fumarate (QTF) and assess the drug's in vitro release mechanism through gastric and intestinal conditions.

Methods A preformulation study was conducted to select the most suitable components and solid-to-liquid lipid ratio for the formulation of nanoparticles. Then, a central composite design was employed to optimize the development of NLC and to study the effect of lipid and surfactant percentages on the physical characteristics of the preparation. The optimal formulation was subjected to physicochemical characterization and stability study. An in vitro release assay using simulated gastrointestinal fluids was performed to study the QTF release mechanism.

Results The optimal formulation showed good particle size, PDI, and zeta potential of 179.2 ± 2.6 nm, 0.220 ± 0.020 , and -33.63 ± 0.23 mV, respectively. The encapsulation efficiency and the loading capacity were $84.49 \pm 1.25\%$ and $2.6 \pm 0.03\%$, respectively. DSC and FTIR analysis showed compatibility between QTF and other components of the formulation and successful encapsulation of the drug within lipid nanoparticles. The optimal formulation also showed good long-term stability at 4 °C storage temperature. The in vitro release of QTF followed the Korsmeyer-Peppas model. The study demonstrated that QTF was mainly released by diffusion mechanism in the gastric medium, and by erosion and anomalous transport in the intestinal medium.

Conclusion NLC represents a suitable formulation for the oral delivery of QTF. Further studies should investigate the oral absorption and lymphatic transport potential of the optimized formulation.

Keywords Nanostructured lipid carriers · Central composite design · Quetiapine fumarate · Release kinetics · Simulated gastrointestinal fluids

Introduction

Schizophrenia and bipolar disorders are two psychotic disorders that deeply influence the life of their victims. These severe and chronic diseases have a big impact on the relations, behavior, and well-being of patients. Many treatments were used to improve the symptoms of these diseases. One of these treatments is quetiapine, an atypical antipsychotic derived from dibenzothiazepine, commercialized as

fumarate salt. Quetiapine fumarate (QTF) is class II in the Biopharmaceutical Classification System (BCS), with good permeability and slight solubility. QTF has better efficacy and better tolerability than classical antipsychotics. It has a clozapine-like activity. Its therapeutic activity is due to the antagonism of neurotransmitter receptors, mainly serotonergic receptor 5HT₂ and dopaminergic receptors D₁ and D₂. It also has a lower affinity to α -adrenergic and muscarinic cholinergic receptors which reduce the cholinergic-like side effects of the molecule [1, 2]. However, after oral absorption, QTF incurs extensive first-pass metabolism by cytochrome CYP P450 3A4. Although it has two active metabolites (7-hydroxy-quetiapine and 7-hydroxy-*N*-desalkylquetiapine), the therapeutic activity is mainly due to the parent molecule [3]. Hence, the improvement of oral bioavailability of QTF and the prolongation of its activity may have a big

✉ Mohamed Ali Lassoued
lassoued98@yahoo.fr

¹ Laboratory of Pharmaceutical, Chemical and Pharmacological Drug Development LR12ES09, Faculty of Pharmacy, University of Monastir, Avicenne Street, 5000 Monastir, Tunisia

interest for patients under chronic treatment of schizophrenia and bipolar disorders. This could be solved by the development of new pharmaceutical forms of the drug that protect it from the first-pass effect and extend its activity. Among these formulations, lipid nanoparticles and nanostructured lipid carriers have gained particular attention in this field.

For a few decades, nanoparticle formulations have been largely studied as new drug delivery systems that improve the absorption and the bioavailability of many drugs. Among these formulations, lipid nanoparticles (LN) represented a very promising system for the delivery of drugs with poor bioavailability. Lipid nanoparticles were firstly developed by Professor RH Muller and are defined as a solid lipophilic matrix with a particle size of 150–300 nm (can reach 50–1000 nm), and in which are incorporated active molecules [4, 5]. The first generation of LN was solid lipid nanoparticles (SLN) which are mainly composed of solid lipid–only matrix. The formulation of these LN is derived from the formulation of oil-in-water nanoemulsions where the liquid lipid in the oil droplets is replaced with solid lipid. These nanoparticles received big attention due to their advantages compared to other organic nanoparticles. SLN presented the benefit to remain solid at the physiologic temperature which gave them better *in vivo* stability [6]. They also give better drug protection and a controlled release of incorporated drugs. The excipients used in these formulations are known for their good tolerability and biodegradability.

Later, a new generation of LN, named nanostructured lipid carriers (NLC), was developed to overcome the limits of SLN [5]. NLC saved the same known benefits of SLN and added more benefits by reducing the crystallinity of the system and improving the drug encapsulation. It has been reported that the perfect crystalline matrix formed in SLN after solidification leads to drug expulsion during storage and lower encapsulation efficiency. However, NLC are composed of a blend of solid and liquid lipid. The addition of liquid lipid creates more imperfections in the lipid crystalline matrix that increases the drug entrapment into the core of nanoparticles and prevents their expulsion during storage [5, 7, 8]. Moreover, the solid matrix of NLC increases the stability of the lipid system and prevents the coalescence that could be observed in classic emulsions [8]. These nanoparticles largely found their application in the oral delivery of drugs. They are reported to enhance the oral bioavailability of poorly soluble drugs [7, 9]. They could protect the active molecules from degradation in the gastrointestinal tract. They also have the potential to target the lymphatic system thanks to their lipid nature [10, 11]. The lymphatic system represents a very interesting way for the oral delivery of many drug compounds since it allows to avoid hepatic first-pass metabolism [9, 12]. It is proven that lipid nanoparticles promote the transport of drugs into the lymphatic system.

Thanks to their lipid nature and small size, lipid nanoparticles can be directly absorbed into the lymphatic circulation [13]. Moreover, the lipid degradation products can be absorbed into the enterocyte and induce the production of chylomicrons. In this case, the lipids and drugs are associated with chylomicrons and directly enter the lymphatic system. The chylomicrons are then transported via the thoracic duct to the subclavian vein where they reach the systemic circulation avoiding the hepatic first-pass metabolism of the associated drugs and extending their circulation time into the blood [13]. Hence, many NLC formulations were developed and proven to enhance the oral bioavailability of several drugs. For example, docetaxel-loaded NLC formulation enhanced the oral bioavailability of docetaxel by 4.31-fold compared to the drug solution [14]. Another study reported that ibrutinib-loaded NLC could achieve an increased bioavailability and lymphatic transport compared to the free drug [15]. Similarly, an anthelmintic drug mebendazole was formulated into NLC, and the formulation showed increased lymphatic passage and avoided the first-pass metabolism of the drug [16].

The aim of this study was to develop a new QTF-loaded NLC for oral delivery, using a quality-by-design approach. A preformulation step was conducted to choose the components used for NLC preparation. Central composite design (CCD) was then used to study the effect of formulation components on the physical properties of NLC, and to select the optimal formulation. The optimal QTF-loaded NLC was then characterized for particle size, polydispersity index (PDI), zeta potential, crystalline state, and drug–excipient compatibility. Moreover, a stability study of the optimal NLC was conducted over one year. Finally, an *in vitro* release study of the novel formulation was assessed in simulated gastro-intestinal fluids to ascertain the drug release mechanism of QTF.

Material and Methods

Chemical Reagents

Quetiapine fumarate (QTF) and Poloxamer 188 were generously provided by “Philadelphia Pharma” laboratories (Sfax, Tunisia). Glycerol monostearate, myristic acid, and oleic acid were purchased from Prolabo® (VWR, France). Stearic acid and soybean lecithin (> 40% phosphatidylcholine) were purchased from Sigma-Aldrich®. Compritol ATO888, Compritol CG888, and Gelucire 43/01 were provided by Gattefosse® (Saint Priest, France). Cetyl alcohol was supplied from AppliChem® (AppliChem GmbH, Germany).

Fasted state simulated gastric fluid (FaSSGF) and fasted state simulated intestinal fluid (FaSSIF) were prepared from simulated intestinal fluid (SIF) instant powder (Phares Drug

Delivery AG, MuttENZ, Switzerland) as indicated by the manufacturer.

Acetonitrile and methanol (HPLC grade) were obtained from Sigma-Aldrich.

Preformulation Study

Selection of Solid and Liquid Lipids

The solubility of QTF in different vehicles was used to identify the suitable solid and liquid lipids that possess good solubilizing capacity for this drug. The selection of liquid lipid for NLC formulation was based on QTF solubility data in various oils as reported in the literature. The selection of solid lipid was determined, experimentally, among several components, viz., glyceryl monostearate, stearic acid, Compritol ATO, Compritol CG, myristic acid, cetyl alcohol, and Gelucire® 43/01. Briefly, 20 mg of QTF was added to a test tube then solid lipid was added in fractions of 200 mg, and the tube was heated to 75 °C under magnetic stirring until the melted lipid became visually clear. The solubility of QTF was calculated based on the amount of lipid added. The assay was conducted in triplicate ($n=3$), and results were expressed as mean \pm SD.

Determination of the Optimal Ratio of Solid to Liquid Lipid

The selected solid and liquid lipids that gave the maximum solubility of QTF were mixed in test tubes at different ratios ranging from 50:50 to 90:10 (w/w) of solid to liquid lipid and maintained under moderate agitation at 80 °C for 1 h. The compatibility of solid lipid and oil was assessed visually by examination of the absence of phase separation at the melted state. Then, the mixtures were allowed to cool down at room temperature. The miscibility of components was assessed by smearing a cooled sample of the mixtures on a filter paper and observing the presence or absence of oil droplets trace on the filter paper.

Determination of the Optimal Drug to Lipid Phase ratio

The solubility of QTF in the optimal lipid mixture was determined empirically. Briefly, 2 g of the lipid phase at the optimal ratio of solid to liquid lipid was prepared and melted at 80 °C. Then, fractions of 2 mg of QTF were added successively to the mixture and kept under magnetic stirring. The addition of QTF was continued until the appearance of opalescence or a precipitate, indicating QTF is not solubilized anymore in the lipid phase. The last fraction was not considered, and the solubility of QTF was calculated based on the penultimate fraction.

Formulation of QTF-Loaded NLC

Preparation of QTF-Loaded NLC

Nanostructured lipid carriers were prepared using hot high shear homogenization followed by solidification at low temperature. Solid lipid and oil were weighed and melted at 80 °C in a water bath under agitation, then QTF was added to the mixture and allowed to agitate until complete solubilization in the lipid phase. Poloxamer 188 and soybean lecithin were used as surfactants at the ratio of 1:1 (w/w). The surfactants were weighed and added to 40 ml of distilled water and heated to the same temperature as the lipid phase. Then, the aqueous phase was added slowly to the melted lipid phase under magnetic stirring to form a coarse emulsion. The coarse emulsion was then homogenized using a high shear homogenizer (Polytron, Kinematica GmbH, Switzerland) at 12,000 rpm at 80 °C for 15 min. The obtained nanoemulsion was passed through a nylon filter membrane of 0.45 μ m pore size and directly injected into 60 ml of cold water (5 °C) and maintained to stabilize under mechanical stirring (Heidolph RZR 2041, Heidolph Instruments GmbH, Germany) at 1200 rpm for 1 h.

Experimental Design

The design of experiments approach was used to optimize the NLC formulation. Two factors of central composite rotatable design (CCD) was chosen for the optimization study. Five levels were defined in the design as $-\alpha$, -1 , 0 , $+1$, and $+\alpha$, with α value equal to 1.414. The independent variables were respectively the percentage of lipid phase (% w/w; X_1) in the preparation and the percentage of surfactants mixture (% w/w; X_2). The low and high levels of each factor were defined based on preliminary studies. Particle size, polydispersity index (PDI), and zeta potential were selected as responses Y_1 , Y_2 , and Y_3 , respectively.

Design-Expert® software (Version 11, Trial version, Stat-Ease Inc., Minneapolis, MN, USA) was used for the statistical analysis. The software generated a total of 13 experiments that included 4 factorial points, 4 axial points, and 5 central point replicates.

The statistical analysis conducted by the Design-Expert software provided the best-fitting mathematical models to establish the polynomial equations for each response. The choice of the model was based on the comparison of several statistical parameters including p -value, lack-of-fit p -value, squared correlation coefficient (R^2), adjusted and predicted R^2 , and the predicted residual sum of square (PRESS). Finally, both independent variables were optimized using the desirability function to establish the optimal NLC formulation.

Physicochemical Characterization

Particle Size, Polydispersity Index, and Zeta Potential Measurements

Particle size, PDI, and zeta potential of NLC preparations were determined using Nanosizer® and Zetasizer® instruments (Nano S and Nano Z, Malvern Instruments, UK), respectively.

The samples were diluted 10 times and 100 times with distilled water before the measurement of the size and the zeta potential, respectively.

All measurements were done in triplicate ($n = 3$) and results were expressed as mean \pm SD.

Encapsulation Efficiency and Drug Loading

The encapsulation efficiency (EE) and drug loading (DL) of the optimal formulation of QTF-loaded NLC were determined, indirectly, by quantifying the amount of drug that was not encapsulated into the nanoparticles. NLC preparation was first diluted with distilled water 20 times, then it was centrifuged at 20 °C for 1 h at 3900 rpm (Roto-fix® 32 A, Andreas Hettich GmbH, Germany) using centrifugal filter tubes (Vivaspin® Turbo 4, MWCO 30 kDa, Sartorius Stedim Lab Ltd., UK). The non-encapsulated QTF present in the filtrate was then determined using HPLC.

The encapsulation efficiency and drug loading of QTF-loaded NLC were calculated using Eq. (1) and Eq. (2) respectively:

$$EE\% = \frac{\text{Total amount of QTF} - \text{Amount of non encapsulated QTF}}{\text{Total amount of QTF}} \quad (1)$$

$$DL\% = \frac{\text{Total amount of QTF} - \text{Amount of non encapsulated QTF}}{\text{Total amount of lipids}} \quad (2)$$

Transmission Electron Microscopy

The morphology of QTF-loaded NLC was studied using transmission electron microscopy (TEM). A drop of NLC sample was diluted in 2 ml of Milli-Q water. Then, a drop-let of the suspension was placed on a carbon-coated copper grid using a micropipette, and the excess liquid was carefully adsorbed on filter paper. The grid was dried at room temperature and observed using a Philips CM-120 Transmission electron microscope (CMEABG, Claude Bernard University Lyon 1, France) by 120 kV accelerating voltage.

Differential Scanning Calorimetry

Thermal characterization of QTF, physical mixture and optimal loaded and unloaded NLC was carried out by differential scanning calorimetry (Mettler Toledo DSC-1). Samples with adequate mass were sealed into aluminum pans and analyzed over a temperature range of 10–300 °C at a heating rate of 10 °C/min.

Fourier Transform Infrared Analysis

FT-IR analysis of the drug, stearic acid, the physical mixture and optimal loaded and unloaded NLC formulations was conducted using FT-IR spectrometer Frontier® (PerkinElmer, France), provided with a diamond horizontal attenuated total reflectance (ATR) sampling accessory. The samples were scanned from 4000 to 6000 cm^{-1} with a resolution of 4 cm^{-1} .

Long-term Physical Stability Study

The physical stability of the optimal NLC formulation was studied over 1 year of storage at two different temperatures (4 °C and room temperature). Particle size, PDI, and zeta potential were determined at different time intervals. All measurements were done in triplicate and results were expressed as mean \pm SD.

In Vitro Drug Release Study

In vitro drug release study was assessed using the dialysis bag method. First, 4 ml of NLC dispersions was placed into a dialysis bag (Spectrum™ Spectra/Por™ 1 RC; 6000 to 8000 MWCO; USA). Next, the latter was placed in a beaker containing 80 ml of release medium kept under gentle stirring (IKA® RH basic 2 hot stirring plate, Germany) at 37 °C. Two different types of media were used to simulate gastrointestinal conditions. The samples were first incubated in simulated gastric fluid (FaSSGF, pH 1.6). After 3 h, the samples were placed into 80 ml of simulated intestinal fluid (FaSSIF, pH 6.5) and kept under stirring at 37 °C for 4 h. Aliquots of 1 ml of the release medium were withdrawn at different time intervals and replaced with an equal volume of fresh medium. The released QTF was then analyzed using HPLC at the wavelength of 250 nm. Results were expressed as mean \pm SD of the percentage of the diffused drug ($n = 3$).

Mathematical Modeling of Release Kinetics

The release data of QTF-loaded NLC was fitted to zero-order, first-order, Higuchi, Hixson-Crowell, and Korsmeyer-Peppas release kinetic models to

evaluate the release mechanism of QTF from NLC in three used media. The analysis was accomplished using the DDSolver® Microsoft Excel add-in program. The adjusted coefficient of determination (R^2_{adjusted}) and Akaike's information criterion (AIC) were both examined to determine the most suitable model [17]. The model that presents the highest coefficient of determination (R^2_{adjusted}) and the lowest AIC values was selected to describe the release mechanism of QTF from nanoparticles [18].

The adjusted coefficient of determination (R^2_{adjusted}) was calculated as follows (Eq. (3)):

$$R^2_{\text{adjusted}} = 1 - \frac{(n-1)}{(n-p)}(1-R^2) \quad (3)$$

n is the number of dissolution data points, and p is the number of parameters in the model.

The AIC was determined using Eq. (4):

$$\text{AIC} = n \cdot \ln(\text{WSS}) + 2 \cdot p \quad (4)$$

n represents the number of data points, WSS is the weighted sum of squares, and p is the number of parameters in the model.

Analytical HPLC Method

The analysis of QTF was done using HPLC Agilent HP 1100 series (Agilent Technologies, Hewlett Packard 1100, Germany) equipped with a photodiode array UV detector, a quaternary pump, a vacuum degasser, and a manual injector G1328A with a 20- μl loop, all from the HP 1100 series. The system was controlled by HP ChemStation® software. The elution was performed using a reverse-phase SUPELCO® C-18 HPLC column (250 mm \times 4.6 mm, 5 μm particle size) as the stationary phase. An isocratic mobile phase composed of acetonitrile (ACN), methanol (MeOH), and 10 mM phosphate buffer K_2HPO_4 (pH 6.5) (50:30:20 v/v/v) was used at a flow rate of 1 ml/min. The selected detection wavelength was 250 nm. The retention time of QTF was 5.45 min.

Statistical Analysis

Statistical analysis was performed using Microsoft® Excel 2016 software and IBM SPSS® Statistics software (version 20; IBM, Armonk, NY, USA). Data were analyzed using a one-way analysis of variance (ANOVA). Tukey, Bonferroni, and Dunnett's two-sided post hoc tests were used to evaluate significant differences. A statistically significant difference was considered when the p -value ≤ 0.05 .

Results and Discussion

Preformulation Study

The preformulation study was conducted to justify the choice of excipients used in the formulation of NLC, precisely the solid and liquid lipid, and to define the best solid-to-liquid lipid ratio that guarantees a better encapsulation of the drug in nanoparticles.

The results of the solubility study of QTF in solid lipids are shown in Fig. 1. Stearic acid, myristic acid, and glyceryl monostearate were the most able to solubilize QTF. Stearic acid gave the best solubility (25 mg/g of solid lipid) compared to other lipids. Hence, stearic acid was chosen as solid lipid in the formulation. For the liquid lipid, the choice was based on earlier studies from the literature. Oleic acid has been reported to give good solubility of QTF [19]. Oleic acid was then selected as liquid lipid.

Further, the optimal ratio of stearic acid to oleic acid was investigated by preparing mixtures of both lipids in different ratios and stirring at a temperature 10 °C above the melting point of stearic acid. The mixtures did not show any phase separation, and both lipids were miscible at the melted state. After cooling, the different mixtures were examined to ensure the encapsulation of the liquid lipid in the lipid mixture. The preparations were smeared on filter paper. The stearic acid: oleic acid ratios from 50:50 and 60:40 (w/w) presented an excess of oil that was absorbed on the filter paper. The ratios from 70:30 to 90:10 (w/w) did not show any oil droplet trace on the filter paper. Therefore, the ratio that contained the higher

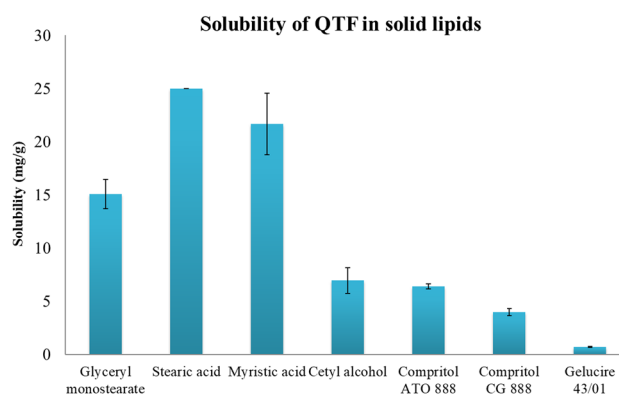


Fig. 1 Solubility of QTF in different solid lipids (data are presented as mean \pm SD, $n = 3$)

amount of liquid lipid and did not show any trace of oil on the filter paper was chosen. The ratio of 70:30 (w/w) was consequently used for the formulation of QTF-loaded NLC.

The solubility of QTF in the selected lipid mixture was then tested. QTF was added to the melted lipid mixture by fractions and was stirred at a temperature 10 °C above the melting point of stearic acid. Fractions were added, and the solubility was assessed visually by the limpid aspect of the mixture. The maximum solubility was appreciated when a precipitate of the drug appeared and persisted after 1 h of agitation. The last fraction added was not considered, and the solubility was calculated based on the dissolved amount of the drug. QTF showed solubility of 32.7 ± 1.15 mg/g of lipid mixture. This value was higher than the value of solubility in stearic acid alone which indicates that the adding of oleic acid increased the solubility of the drug in the lipid mixture and allowed to encapsulate an increased amount of QTF. The choice of the initial loading percentage of the drug is a determining parameter in the formulation. The initial loading percentage should be lower than the solubility of the drug in melted lipid because this solubility would decrease upon cooling and solidification of lipids, and may result in drug expulsion [4]. Hence, the initial loading percentage of QTF in NLC was set at 3% (w/w) of the lipid mixture to ensure the solubilization of the total amount of the drug in the lipid phase.

Poloxamer 188 and soybean lecithin were used as surfactant and co-surfactant, respectively, in the formulation of NLC at the ratio 1:1 based on previous work and preliminary studies (Data not shown) [20, 21].

Formulation and Optimization of QTF-Loaded NLC

Central Composite Design: Statistical Analysis

CCD experimental design was conducted to optimize the formulation of QTF-loaded NLC. A two-factor five-level rotatable CCD was employed to optimize the prepared NLC. The percentage of total lipids (X_1) and the percentage of surfactant (X_2) were defined as independent variables. The

low and high levels ($-\alpha, -1, 0, 1, +\alpha$) of each independent factor are resumed in Table 1 and were defined based on preliminary studies.

The experimental design software (Design-Expert® Version 11, Trial version) generated 13 experiments that were realized as described above. The matrix of experiments and the results of dependent variables for each experiment are presented in Table 2.

The results were analyzed to determine the best-fitting model for each response based on several parameters. A good-fitting mathematical model should have a significant p -value with the highest R^2 value and not a significant lack of fit p -value. The difference between predicted R^2 and adjusted R^2 is less than 0.2, and the adequate precision value is more than 4 which means an acceptable signal-to-noise ratio.

Analysis of variance (ANOVA) was conducted to evaluate the significance of each regression coefficient in the model. The resulted polynomial equations only used the coefficients of variables that have a significant p -value (< 0.05). Particle size (Y_1) response fitted a linear model ($R^2 = 0.925$), PDI (Y_2) response fitted a quadratic model ($R^2 = 0.972$), and zeta potential (Y_3) response fitted a two-factor interaction (2FI) model ($R^2 = 0.967$) signifying a good correlation between the studied variables and the obtained response values. The results of the best-fitting models and the corresponding polynomial equation of each response are resumed in Table 3. Three-dimensional response surface plots were established to determine the effect of each independent variable on response results (Fig. 2).

Effect of Independent Variables on Particle Size

Particle size values varied between 152.2 and 384.8 nm. The results fitted a linear model and generated the mathematical equation presented in Table 3. ANOVA results showed that both independent variables have a significant effect on particle size (Table 4). From the 3D plots of particle size response (Fig. 2a), it can be seen that the size of particles increases when lipid concentration decreases and surfactant concentration increases.

The negative value (-34.84) before factor X_1 means a negative effect of the total lipid concentration on particle

Table 1 Independent and dependent variables of CCD

Factor	Predefined levels				
	$-\alpha$	Low (-1)	Center (0)	High ($+1$)	$+\alpha$
Independent variables					
Percentage of total lipids (%) X_1	0.4	0.546	0.9	1.253	1.4
Percentage of surfactant mixture (%) X_2	0.2	0.317	0.6	0.88	1
Dependent variables	Goals				
Particle size (nm) Y_1	Minimize				
PDI Y_2	Minimize				
Zeta potential (mV) Y_3	In range ($> 30 $)				

Table 2 Experimental matrix of CCD and observed results of each response

Run	Input		Output		
	Factor 1	Factor 2	Response 1	Response 2	Response 3
	X ₁ : lipid phase	X ₂ : Surfactant	Particle size	PDI	Zeta potential
Unit	%	%	nm		mV
1	1.254	0.317	152.2	0.245	−32.5
2	0.900	0.600	227.7	0.229	−36.2
3	0.400	0.600	299.3	0.475	−36.2
4	1.400	0.600	197.4	0.285	−35.4
5	1.254	0.883	310.8	0.484	−38.4
6	0.546	0.317	212.8	0.203	−36.1
7	0.900	0.600	237.9	0.268	−36.2
8	0.900	0.200	169.3	0.200	−34.3
9	0.900	0.600	275.5	0.276	−35.8
10	0.546	0.883	384.8	0.606	−35.7
11	0.900	0.600	264.2	0.284	−36.2
12	0.900	0.600	263.8	0.262	−36.2
13	0.900	1.000	324.6	0.596	−38.3

size [22]. These results are not very convenient with earlier similar studies. An increase in lipid concentration will increase the viscosity of the preparation and lead to larger particle size by increasing the collisions and aggregation between particles [23, 24]. However, some studies reported the same phenomenon with a decrease in particle size when increasing the lipid concentration. The cause of this observation is not well elucidated, but Vitorino et al. [25] suggested that this increase in particle size could be due to a deficient dispersion when lipid phase concentration is very low.

On the other hand, the positive value (68.78) before factor X₂ indicated a positive effect of surfactant concentration on particle size. Poloxamer 188 and soy lecithin were used as surfactant and co-surfactant for the preparation of NLC. The concentration of surfactant in the preparation has an important impact on particle size. Surfactants are employed to reduce the interfacial tension between the lipid phase and aqueous phase and hence facilitate the formation of small particles [26, 27]. At optimal concentration, molecules of surfactant will form a thin film to cover the entire surface of nanoparticles, allowing to reduce the size of particles and prevent their aggregation. However, when exceeding this optimal concentration, surfactant molecules will accumulate

on the surface of nanoparticles and lead to excessive coverage of crystallized nanoparticles and raising of their size [22, 23, 28].

Effect of Independent Variables on PDI

PDI is the parameter that measures the degree of heterogeneity of the size distribution of nanoparticles. PDI is a dimensionless index whose values could vary between 0.0 (highly monodisperse size distribution) and 1.0 (multiple size populations with very polydisperse distribution) [29]. In the case of lipid nanoparticles, values under 0.3 are considered to be acceptable and reflect a homogenous size distribution, and values higher than 0.5 are considered polydisperse [30]. A homogenous distribution and a low PDI value are suitable to ensure the stability of the preparation and prevent particle aggregation.

The 3D plot of the effect of independent variables on PDI is presented in Fig. 2b. The graph showed an increase in PDI when the surfactant concentration increases. PDI values ranged from 0.200 to 0.606. In the polynomial equation, the most influencing factor on PDI value is factor X₂ with a positive effect (value before the factor is the biggest = 0.15

Table 3 Best-fit models and polynomial equations for each response

Response	Selected model	R ²	Polynomial equation
Particle size (nm)	Linear	0.9252	$Y_1 = 255.41 - 34.84 X_1 + 68.78 X_2$
PDI	Quadratic	0.9722	$Y_2 = 0.26 - 0.044 X_1 + 0.15 X_2 - 0.041 X_1 X_2 + 0.057 X_1^2 + 0.066 X_2^2$
Zeta potential (mV)	2FI	0.9673	$Y_3 = -35.96 + 0.25 X_1 - 1.39 X_2 - 1.58 X_1 X_2$

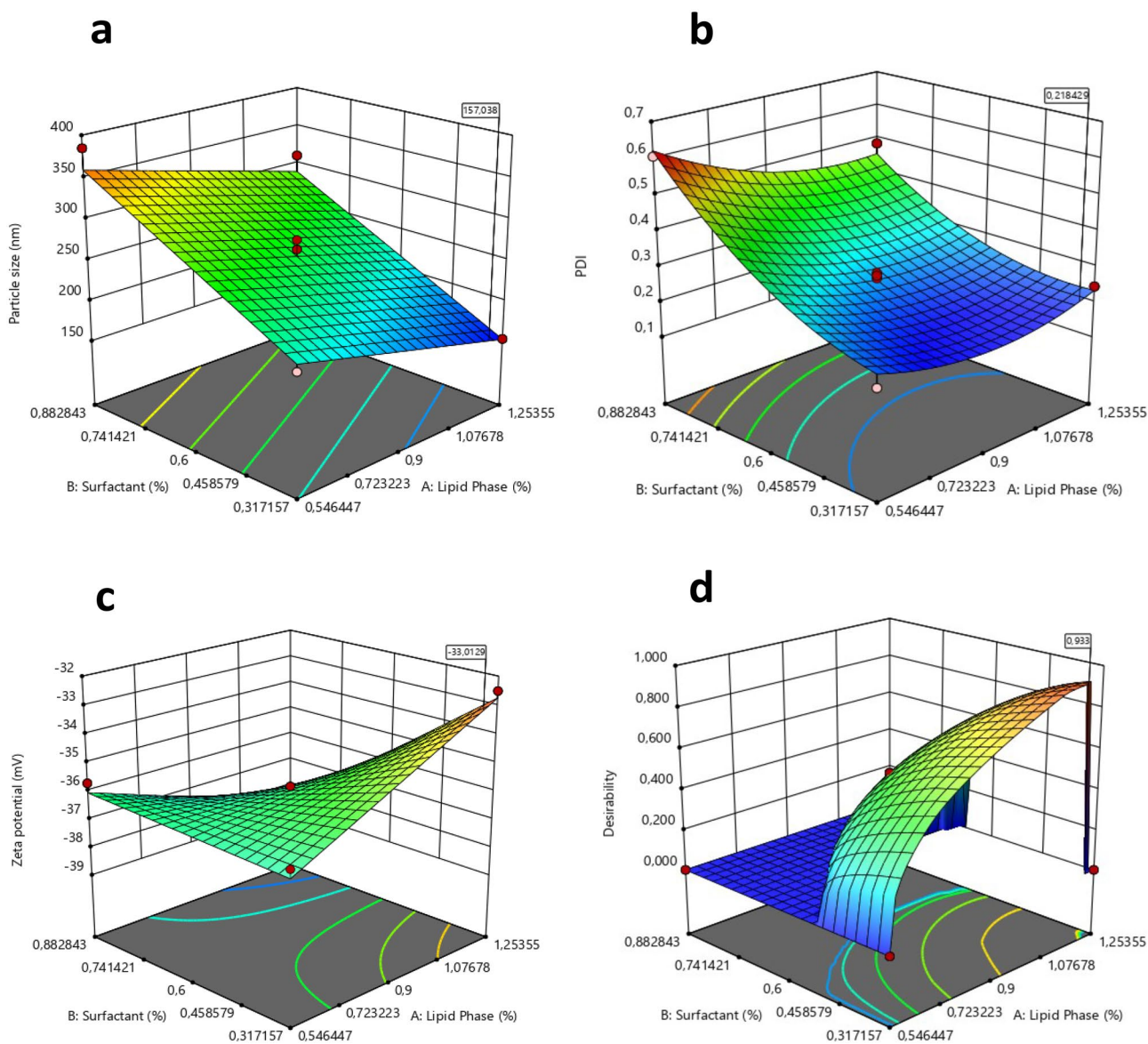


Fig. 2 3D response surface plots showing the effect of independent variables on **a** particle size, **b** PDI, **c** zeta potential, **d** desirability

with p -value < 0.0001). This increase in PDI indicates a less homogeneous size distribution of particles present in the preparation. It could be due to an excess coverage at

the surface of the nanoparticles by surfactant molecules. An excess of lecithin may conduct to the formation of a double layer and hence increases the size of particles [31].

Table 4 Summary ANOVA for the selected model for the measured responses

Parameters	Y1: particle size		Y2: PDI		Y3: zeta potential	
	Source	P -value	Source	P -value	Source	P -value
Model	Linear	< 0.0001	Quadratic	< 0.0001	2FI	< 0.0001
Intercept	255.41		0.26		-35.96	
X_1	-34.84	0.0005	-0.044	0.0062	0.25	0.0481
X_2	68.78	< 0.0001	0.15	< 0.0001	-1.39	< 0.0001
X_1X_2			-0.041	0.0369	-1.58	< 0.0001
X_1^2			0.057	0.0022		
X_2^2			0.066	0.0009		

Moreover, at a higher concentration, free Poloxamer 188 molecules could form self-micelles with a lower particle size which contributes to the increase of PDI value [32].

Effect of Independent Variables on Zeta Potential

Zeta potential values varied between -36.2 and -32.5 mV indicating the formed nanoparticles were negatively charged. This parameter measures the surface charge representing the electrostatic forces of repulsion and attraction between nanoparticles. A high value of zeta potential $>|30|$ mV indicates good electrostatic repulsive forces and hence the stabilization of nanoparticles and prevention of their aggregation under storage [33]. From the polynomial equation of zeta potential response (Table 3) and the corresponding 3D plot (Fig. 2c), the surfactant concentration and the interaction between lipid phase and surfactant are the most influencing factors on the response. Negative values before factor X_2 (-1.39) and factor X_1X_2 (-1.58) with significant p -values (<0.0001) indicate synergic effects increasing the negative value of zeta potential. The choice of surfactant is a primordial parameter in the formulation of NLC. Here, both Poloxamer 188 and soybean lecithin were used as surfactants to stabilize the formulation, and they both resulted in an anionic charge on the surface of nanoparticles. The reason for this charge could be attributed to the negatively charged phospholipids present in lecithin [31, 34, 35]. Moreover, poloxamer molecules could be polarized and adsorb the charge in water which results in the formation of an electric double layer similar to ionic at the interface between particles and water [36].

Optimization of QTF-Loaded NLC

The optimization of QTF-loaded NLC formulation was obtained numerically using the desirability function of Design-Expert® software. The numerical optimization of the independent variables is based on the combination of all the responses in only one measure to allow the prediction of an optimum value for each independent variable. In our case, we aimed to minimize particle size and PDI. Zeta potential values were acceptable values for all responses (less than -30 mV), so the zeta potential response was set to be in range. We also aimed to maximize the lipid phase and minimize the surfactant percentage.

The optimum solution provided by the experimental design software was composed of 1.2% of total lipids and 0.317% of surfactant mixture (Fig. 2d). The predicted responses for particle size, PDI, and zeta potential were respectively 157.03 nm, 0.218, and -33.012 mV. The desirability value was 0.933.

To validate the model, the optimal formulation was prepared and checked for each response ($n = 3$). The observed

values of particle size, PDI, and zeta potential were respectively 179.2 ± 2.68 nm, 0.220 ± 0.02 , and -33.63 ± 0.23 mV (Table 5). These results were statistically comprised into the prediction intervals given by the software which means the model is validated and can correctly predict the optimal formulation results.

Physicochemical Characterization of Optimal QTF-Loaded NLC

The results of characterization for particle size, PDI, and zeta potential are shown in Table 5.

The optimal formulation exhibited particle size less than 300 nm which is suitable for intestinal transport and oral delivery [37]. PDI values showed a good and homogenized distribution of the size of nanoparticles (value <0.3). Zeta potential values indicated negatively charged NLC. The high values of zeta potential (more than ± 30 mV) indicate good stability of the preparation due to electrostatic repulsive forces between charged nanoparticles and prevent their aggregation [38].

Furthermore, the optimal formulation showed good entrapment efficiency ($84.49 \pm 1.25\%$) and loading capacity ($2.6 \pm 0.03\%$). As mentioned by Muchow et al. [39], the loading capacity depends on the solubility of the drug in the lipid blend. NLC are known to have a better encapsulation capacity of drugs than solid lipid nanoparticles (SLN) due to the incorporation of liquid lipid. The liquid lipid reduces the crystallinity of the lipid matrix, creating more imperfections in the crystal and allowing better entrapment of the drug molecules [40, 41]. In our study, the initial loading of NLC was 3% (w/w) of the total lipid phase. This percentage was fixed based on the solubility of QTF in the melted lipid mixture. The loading capacity was close to the initial loading indicating that QTF was well encapsulated into lipid nanoparticles.

Transmission Electron Microscopy

The morphology of the developed NLC was examined using transmission electron microscopy. The micrograph of nanoparticle suspension (Fig. 3) revealed well-individualized particles with a pseudospherical shape. However, the size of nanoparticles was increased compared to the Nanosizer

Table 5 Observed and predicted values of optimal NLC formulation

Response	Predicted value	Observed value ($n = 3$; mean \pm SD)	% variation
Particle size (nm)	157.03	179.2 ± 2.68	12.37
PDI	0.218	0.220 ± 0.02	0.9
Zeta potential (mV)	-33.012	-33.63 ± 0.23	1.84

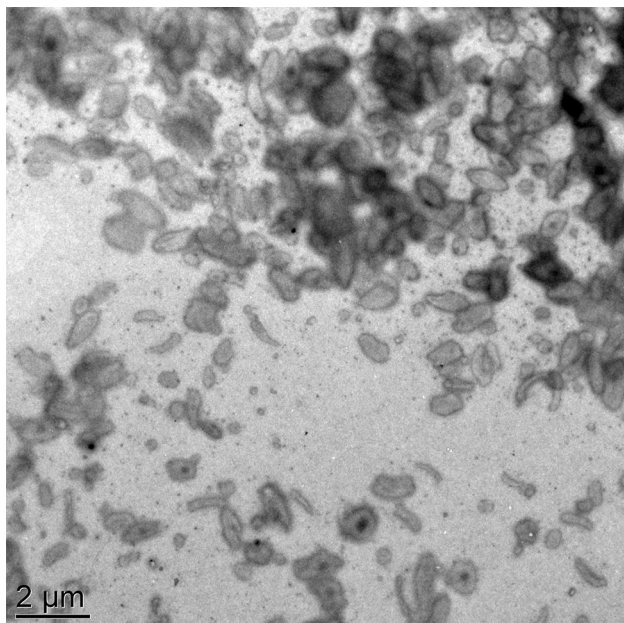


Fig. 3 Transmission electron micrograph of QTF-loaded NLC formulation

measurement results. Also, an agglomeration of nanoparticles was observed. This could be explained by structural changes in the shape of nanoparticles due to dehydration and sample drying [6]. It could be also due to the time between preparation and analysis of the samples that were stored at

room temperature, causing an agglomeration and increase in particle size.

Differential Scanning Calorimetry

Results of DSC analysis are shown in Fig. 4. DSC thermogram of QTF showed an endothermic peak at 174 °C indicating the crystalline nature of the drug. Blank NLC and QTF-loaded NLC showed endothermic peaks at 55 °C and 54.7 °C, respectively. The melting temperature of NLC is above 40 °C which confirms the solid state of the formed nanoparticles at room temperature and physiological temperature. This result is convenient with the definition of NLC which are solid nanoparticles with reduced crystallinity.

The peak of QTF did not appear on the QTF-loaded NLC thermogram which could mean QTF was dissolved into melted lipids and is present in amorphous form. The peak of the physical mixture of the lipids and the drug was decreased (49 °C) compared to the peaks of charged and blank NLC. This may be due to the preparation processes of nanoparticles [42].

Fourier Transform Infrared Analysis

Figure 5 shows the FTIR spectrum of QTF, stearic acid, blank NLC, and QTF-loaded NLC. QTF presented characteristic peaks at 649–662 cm^{-1} (C–S–C stretching), 767–794 cm^{-1} (disubstituted aromatic C–H), 1064 cm^{-1}

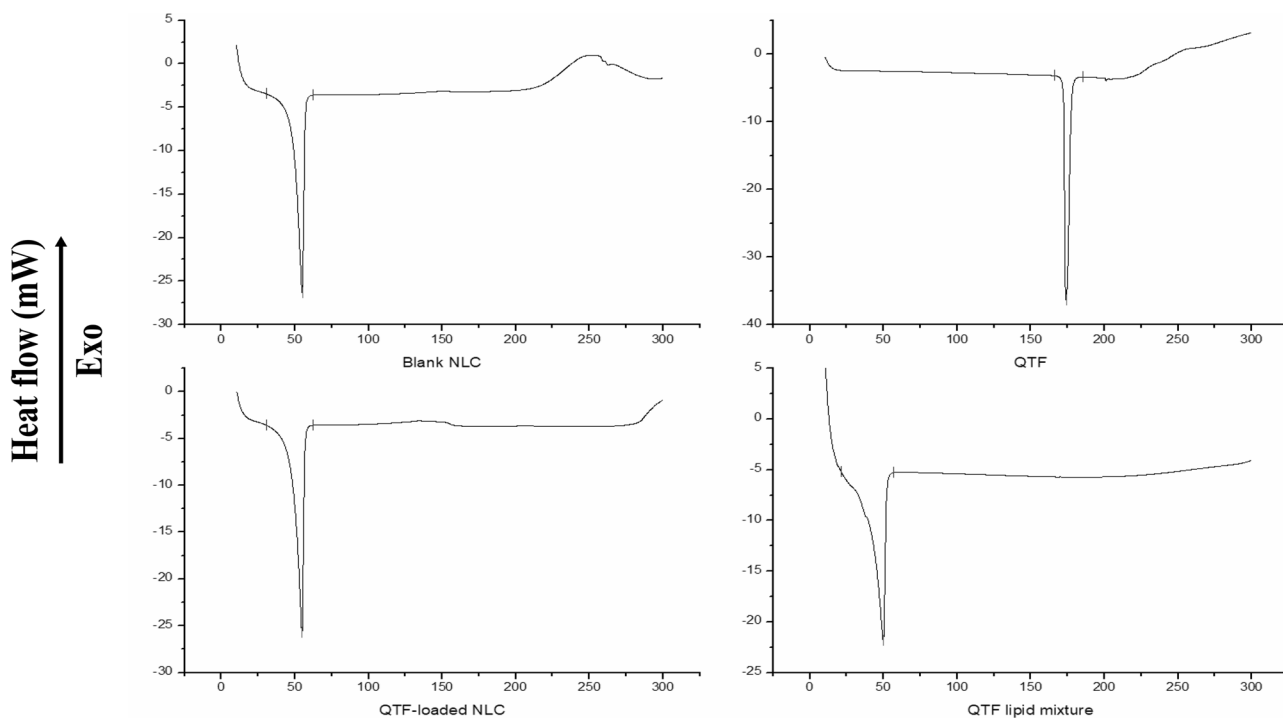
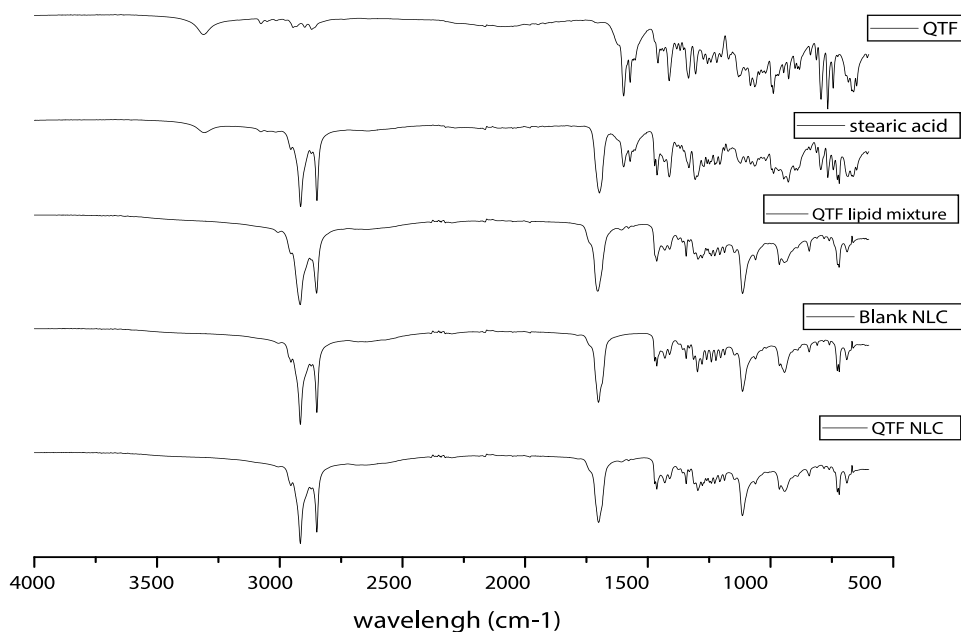


Fig. 4 DSC thermograms of QTF, QTF lipid mixture, blank NLC, and QTF-loaded NLC

Fig. 5 FTIR spectrum of QTF, stearic acid, QTF lipid mixture, blank NLC, QTF-loaded NLC



(C–O–C symmetrical stretching), 1413 cm^{-1} (C–H bending), 1599 cm^{-1} (C=N stretching), $2898\text{--}2946\text{ cm}^{-1}$ (C–H stretching), and 3311 cm^{-1} (O–H stretching) [42, 43]. Stearic acid showed peaks at $1307\text{--}1462\text{--}1698\text{ cm}^{-1}$ referring to the COOH group, $2848\text{--}2915\text{ cm}^{-1}$ (CH_2 stretching), and 3309 cm^{-1} (O–H stretching) [44]. Blank NLC and QTF-loaded NLC showed characteristic peaks of stearic acid and a characteristic peak at 1114 cm^{-1} which could be due to the presence of Poloxamer 188 (C–O stretching). QTF characteristic peaks were absent in the QTF-loaded NLC spectrum which indicates successful encapsulation of the drug into the nanoparticles.

Long-term Physical Stability Study

The results of the stability study of NLC formulation upon 1 year of storage are presented in Fig. 6. The increase in particle size and PDI was more pronounced upon storage at room temperature compared to NLC stored at 4°C . After 3 months, particle size and PDI values were respectively $241.8 \pm 4.4\text{ nm}$ and 0.266 ± 0.015 at 4°C , and $388 \pm 10.9\text{ nm}$ and 0.430 ± 0.033 at room temperature.

After 1 year of storage, particle size and PDI showed a significant increase ($p < 0.05$). However, at 4°C , particle size remained below 300 nm ($293.7 \pm 3.5\text{ nm}$) and PDI was 0.305 ± 0.005 . Thus, the preparation was still suitable for oral delivery [9, 30, 37]. Contrarily, preparations that were stored at room temperature underwent a more significant increase in particle size ($> 500\text{ nm}$) and gave a higher PDI value (0.614 ± 0.072). Despite the increase of particle size and PDI, zeta potential values did not incur significant modifications over 1 year of storage at both temperatures

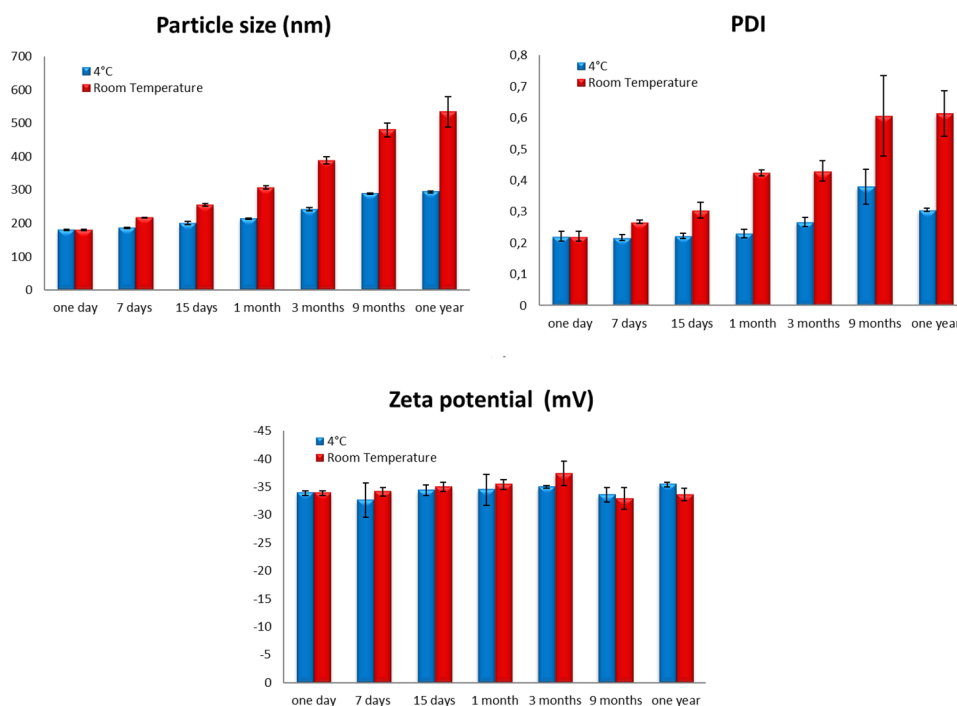
($p > 0.05$). The effect of temperature on the stability of lipid nanoparticles was previously investigated, and similar results have been found [15, 45, 46]. Studies indicated that the increase in particle size could be due to gel formation and lipid transformation. The lipids in NLC formulation are mainly present under β' and α polymorphs, and during storage, they will progressively transform to more stable β polymorphs leading to gel formation [33, 37]. Moreover, the Poloxamer 188 gelling effect could also contribute to particle aggregation by forming a network structure between nanoparticles [33]. These transformations could be retarded by storage under low temperatures allowing better stability of the formulation [33]. A previous study of QTF-loaded NLC composed of Precirol and oleic acid as lipid phase has reported similar findings where particle size and PDI increased significantly upon 3 months of storage. The increase was more pronounced at room temperature than at $5 \pm 3^\circ\text{C}$ which is in good correlation with our findings [47]. The stability study results suggest that the NLC formulation should be stored at 4°C to prevent particle size growth during storage.

In Vitro Drug Release Study

The in vitro release study of QTF from the optimized formulation of NLC was conducted using the dialysis membrane technique. Simulated gastrointestinal fluids were used as release media to investigate the release mechanism of the drug and predict the fate of NLC in physiologic conditions.

The release profile of QTF-loaded NLC is presented in Fig. 7. The optimal formulation of NLC was first incubated for 3 h in the FaSSGF (pH 1.6) to simulate the passage

Fig. 6 Stability study of optimal NLC formulations (data are reported as mean \pm SD of 3 measurements, $n = 3$)



through the gastric conditions. In the acidic medium, QTF presented a relatively high diffusion rate ($63.52 \pm 1.88\%$ in 3 h). After 3 h, samples were transferred to the FaSSIF medium (pH 6.5) and incubated for four hours. The release of QTF from NLC in FaSSIF was significantly slower than in FaSSGF (only 11.45% released in FaSSIF within 4 h). At the end of the assay, the cumulative release of QTF from NLC was $74.98 \pm 0.89\%$.

From the release curve, it can be observed that QTF exhibited a biphasic release profile with faster release in FaSSGF and slower release in FaSSIF. The first rapid release of the drug could be explained by the chemical nature of QTF which has a pH-dependent solubility with higher solubility in acidic media [48]. This first release could be also attributed to the diffusion of the non-encapsulated drug, or to the release of drug molecules that are solubilized in the liquid lipid of the outer shell layer of nanoparticles [49]. The liquid lipid in the formulation reduces the density of the lipid matrix and makes it more permeable, which facilitates drug release. The ratio of solid to liquid lipid in our formulation was 70:30 (w/w). In a previous study, Agarwal et al. developed an NLC formulation of QTF with a solid-to-liquid lipid ratio of 84:16. They found that the first release at pH 1.2 was only 21% within 2 h which confirms the role of liquid lipid to facilitate the release of the drug [47]. The first burst release could be also due to the use of FaSSGF instead of hydrochloric acid solution 0.1 N. The phospholipids and natural surfactants present in FaSSGF may enhance the release of QTF from nanoparticles.

In the simulated intestinal medium, the optimized formulation allowed a controlled prolonged release of QTF from

nanoparticles. This could be due to a slower release of the drug from the lipid matrix or a reduction of its solubility at the intestinal pH 6.5.

Since the developed formulation is intended to improve the intestinal lymphatic transport of QTF, the fast release of the drug in the FaSSGF could be a limiting factor to lymphatic transport. However, the presence of long-chain fatty acids (stearic acid and oleic acid) in the gastrointestinal environment could still affect the *in vivo* fate of the drug [50].

It has been reported that after oral administration, the lipids undergo partial digestion in the stomach by the gastric lipase [13, 51]. At this stage, free drug molecules can be still incorporated into the coarse emulsion formed by the lipid digestion products and gastric fluid, and transported to the small intestine. In the small intestine, the formed coarse emulsion is reduced into small micelles and mixed micelles under the effect of bile salts and other enzymes, which will then be absorbed by the enterocytes.

The use of long-chain fatty acids would promote the production of chylomicrons and improve the transport of the drug to the lymphatic system [13, 51].

Moreover, the NLC, being lipid nanoparticles, present good bioadhesive properties which would delay their stay in the small intestine [52, 53]. The bioadhesion of NLC to the intestinal wall would prolong the residence time of NLC in the intestinal tract and hence allow nanoparticles to release the drug directly to the enterocytes. It was also reported that nanoparticles could be directly absorbed into the lymphatic system via paracellular or transcellular transport [12].

IN VITRO DRUG RELEASE

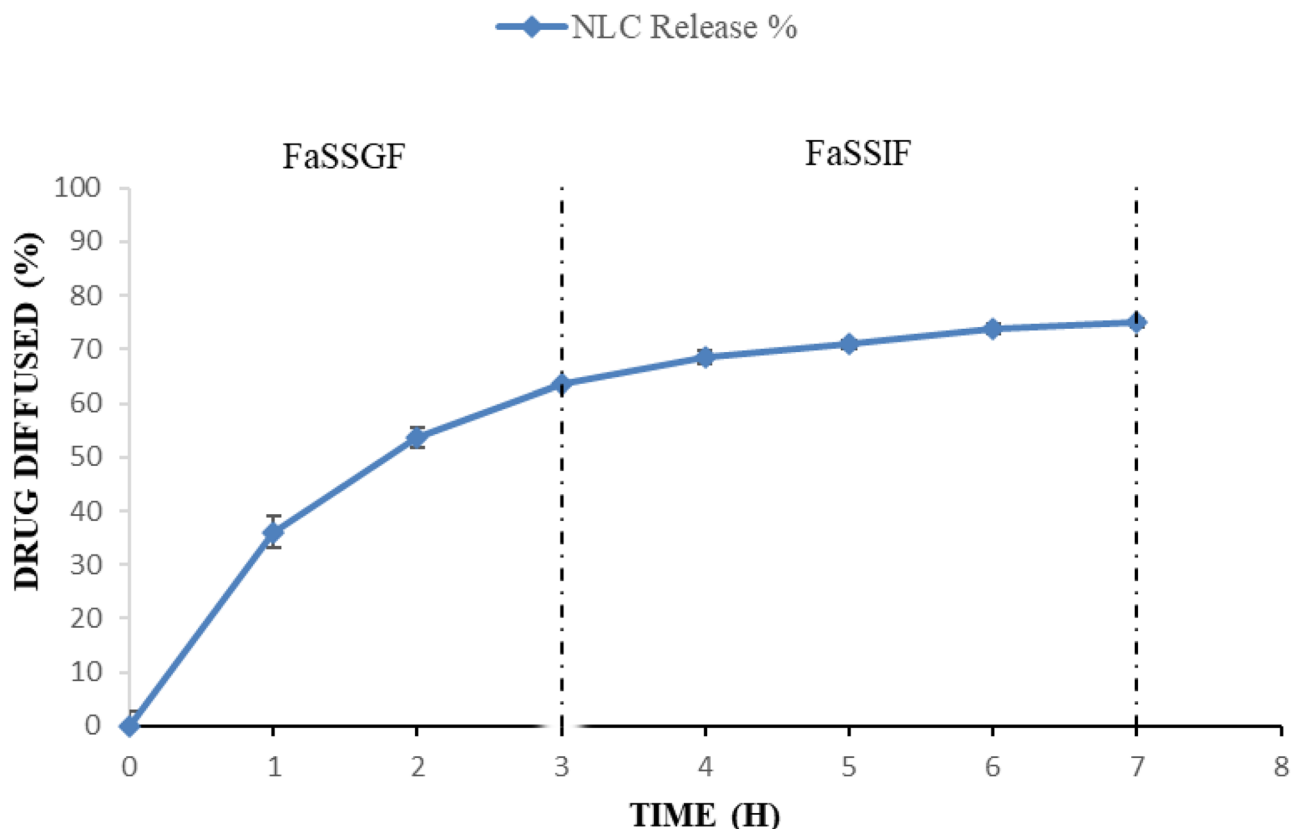


Fig. 7 In vitro dialysis bag drug release of QTF and QTF-loaded NLC (data are expressed as mean \pm SD, $n = 3$)

Mathematical Modeling of the Release Kinetics

To explore the release mechanism of the drug in each medium, the release data were fitted to various kinetic mathematical models. Since two different media were used in the release study, it was more suitable to examine the release mechanism of each media apart. Hence, the release kinetic models (zero-order, first-order, Higuchi, Hixson-Crowell, and Korsmeyer-Peppas) were applied to a 3-h release profile in FaSSGF (Online Resource 1) and 4-h release profile in FaSSIF (Online Resource 2), and not to the total duration of the assay. The calculated coefficients R^2_{adjusted} and AIC values are presented in Table 6. For the gastric medium, the release data fitted well to Higuchi and Korsmeyer-Peppas models with R^2_{adjusted} of 0.986 and 0.983 respectively. However, when checking the AIC values, the Korsmeyer-Peppas model gave the lowest AIC of 6.469 compared to 6.523 in the Higuchi model. In the intestinal medium, the best fitting model was Korsmeyer-Peppas with the highest R^2_{adjusted} (0.979) and the lowest AIC (-2.243).

Table 6 Results of R^2 coefficients obtained after fitting data release of QTF-loaded NLC to different kinetic models

Models	Parameters	FaSSGF pH 1.6	FaSSIF pH 6.5
Zero order	R^2_{adjusted}	0.323	0.757
	AIC	18.53	9.205
	k_0	23.858	3.202
First order	R^2_{adjusted}	0.887	0.799
	AIC	12.99	8.406
	k_1	0.377	0.034
Higuchi	R^2_{adjusted}	0.986	0.954
	AIC	6.523	1.982
	k_H	37.005	5.590
Hixson-Crowell	R^2_{adjusted}	0.767	0.786
	AIC	15.258	8.678
	k_{HC}	0.108	0.011
Korsmeyer-Peppas	R^2_{adjusted}	0.983	0.979
	AIC	6.469	-2.243
	k_{KP}	36.825	4.917
	n	0.508	0.624

R^2_{adjusted} adjusted coefficient of determination, AIC Akaike's information criterion, k_0 release constant of the zero-order model, k_1 release constant of the first-order model, k_H release constant of the Higuchi model, k_{HC} release constant of the Hixson-Crowell model, k_{KP} release constant of the Korsmeyer-Peppas model, n release exponent

The Korsmeyer-Peppas model equation is expressed as follows (Eq. (5)):

$$\frac{Q_t}{Q_\infty} = k.t^n \quad (5)$$

where Q_t/Q_∞ is the fraction of the drug released at time t , and n is the release exponent that characterizes different release mechanisms including Fickian and non-Fickian diffusion. When the n value is less than 0.5, the release of the drug happens mainly by the Fickian diffusion mechanism. The n value indicates a super case II transport when it is higher than 1 and a case II transport when it is equal to 1. A value comprised between 0.5 and 1 indicates anomalous transport and non-Fickian diffusion [17, 18].

In our study, the n value of the Korsmeyer-Peppas model was checked for each medium apart to compare the release mechanism in both media. The n values were 0.508 and 0.624, respectively, for FaSSGF and FaSSIF. Values were comprised between 0.5 and 1 for both media, indicating that the drug release was governed by anomalous transport and non-Fickian diffusion [54, 55]. The anomalous transport means that the release can occur by diffusion, swelling, or erosion [49].

In the case of FaSSGF, it can be remarked that the n value is closer to 0.5, which confirms that the first release of QTF was dominated by diffusion from the outer shell of nanoparticles and in less importance, by partial erosion due to the surfactants and phospholipids present in the medium [56]. However, in the FaSSIF medium, the release is more likely to follow an erosion mechanism. The presence of bile salts and natural surfactants at a higher concentration in FaSSIF could partially and slowly degrade nanoparticles due to the digestion process and would contribute to the release of QTF [9].

Conclusion

QTF-loaded NLC formulation was successfully developed and optimized in this study. CCD design was used to investigate the effects of components ratio on the physical characteristics of NLC and to select the optimum formulation composition. The optimal formulation was then characterized. The particle size, PDI, and zeta potential of optimal formulation were respectively 179.2 ± 2.68 nm, 0.220 ± 0.02 , and -33.63 ± 0.23 mV. The NLC formulation also exhibited good encapsulation efficiency ($84.49 \pm 1.25\%$) and good long-term stability when conserved at 4 °C. In vitro drug release of QTF-loaded NLC showed faster release in gastric fluid FaSSGF compared to intestinal fluid FaSSIF. The kinetics of the release profile was investigated and results showed that QTF release followed the Korsmeyer-Peppas

model indicating mainly non-Fickian anomalous diffusion of the drug.

Hence, the developed NLC formulation can be considered suitable for oral administration and further studies are being conducted to investigate the oral absorption potential and the intestinal lymphatic transport of the drug to improve its oral bioavailability.

Supplementary Information The online version contains supplementary material available at <https://doi.org/10.1007/s12247-021-09567-0>.

Acknowledgements The authors acknowledge Professor Hatem Fessi from the laboratory LAGEP-UMR 5007 (Claude Bernard University Lyon 1, France) for his help in TEM analysis. The authors also acknowledge Professor Salette Reis and Cláudia Nunes from the laboratory REQUIMTE (Faculdade de Farmácia, Universidade do Porto, Portugal) for providing the simulated intestinal fluids powder and for their help with FTIR analysis.

Author Contribution O.B.H.A., M.A.L., and S.S. conceived and designed the experiment. O.B.H.A. performed the experimental work. O.B.H.A. and M.A.L. analyzed the experimental results. O.B.H.A. and M.A.L. wrote the paper. All the authors reviewed the paper.

Declarations

Conflict of Interest The authors declare no competing interests.

References

- DeVane CL, Nemeroff CB. Clinical pharmacokinetics of quetiapine. *Clin Pharmacokinet*. 2001;40(7):509–22. <https://doi.org/10.2165/00003088-200140070-00003>.
- Sanford M, Keating GM. Quetiapine. *CNS Drugs*. 2012;26(5):435–60. <https://doi.org/10.2165/11203840-000000000-00000>.
- Cheer SM, Wagstaff AJ. Quetiapine. *CNS Drugs*. 2004;18(3):173–99. <https://doi.org/10.2165/00023210-200418030-00004>.
- Müller RH, Mäder K, Gohla S. Solid lipid nanoparticles (SLN) for controlled drug delivery – a review of the state of the art. *Eur J Pharm Biopharm*. 2000;50(1):161–77. [https://doi.org/10.1016/S0939-6411\(00\)00087-4](https://doi.org/10.1016/S0939-6411(00)00087-4).
- Rainer HM, Ranjita S, Cornelia MK. 20 years of lipid nanoparticles (SLN & NLC): present state of development & industrial applications. *Curr Drug Discov Technol*. 2011;8(3):207–27. <https://doi.org/10.2174/157016311796799062>.
- Beloqui A, Solinís MÁ, Rodríguez-Gascón A, Almeida AJ, Préat V. Nanostructured lipid carriers: promising drug delivery systems for future clinics. *Nanomedicine: Nanotech Bio Med*. 2016;12(1):143–61. doi:<https://doi.org/10.1016/j.nano.2015.09.004>.
- Beloqui A, del Pozo-Rodríguez A, Isla A, Rodríguez-Gascón A, Solinís MÁ. Nanostructured lipid carriers as oral delivery systems for poorly soluble drugs. *Journal of Drug Delivery Science and Technology*. 2017;42:144–54. <https://doi.org/10.1016/j.jddst.2017.06.013>.
- Ganesan P, Narayanasamy D. Lipid nanoparticles: different preparation techniques, characterization, hurdles, and strategies for the production of solid lipid nanoparticles and nanostructured lipid carriers for oral drug delivery. *Sustain Cities Soc*. 2017;6:37–56. <https://doi.org/10.1016/j.scp.2017.07.002>.

9. Poonia N, Kharb R, Lather V, Pandita D. Nanostructured lipid carriers: versatile oral delivery vehicle. *Future Science OA*. 2016;2(3):FSO135. <https://doi.org/10.4155/fsoa-2016-0030>.
10. Lawless E, Griffin BT, O'Mahony A, O'Driscoll CM. Exploring the impact of drug properties on the extent of intestinal lymphatic transport - in vitro and in vivo studies. *Pharm Res*. 2015;32(5):1817–29. <https://doi.org/10.1007/s11095-014-1578-x>.
11. Chaturvedi S, Garg A, Verma A. Nano lipid based carriers for lymphatic voyage of anti-cancer drugs: an insight into the in-vitro, ex-vivo, in-situ and in-vivo study models. *J Drug Delivery Sci Technol*. 2020;59: 101899. <https://doi.org/10.1016/j.jddst.2020.101899>.
12. Pandya P, Giram P, Bhole RP, Chang HI, Raut SY. Nanocarriers based oral lymphatic drug targeting: strategic bioavailability enhancement approaches. *J Drug Delivery Sci Technol*. 2021;102585. <https://doi.org/10.1016/j.jddst.2021.102585>.
13. Poovi G, Damodharan N. Lipid nanoparticles: a challenging approach for oral delivery of BCS Class-II drugs. *Future J Pharm Sci*. 2018;4(2):191–205. <https://doi.org/10.1016/j.fjps.2018.04.001>.
14. Fang G, Tang B, Chao Y, Zhang Y, Xu H, Tang X. Improved oral bioavailability of docetaxel by nanostructured lipid carriers: in vitro characteristics, in vivo evaluation and intestinal transport studies. *RSC Adv*. 2015;5(117):96437–47. <https://doi.org/10.1039/C5RA14588K>.
15. Rangaraj N, Pailla SR, Shah S, Prajapati S, Sampathi S. QbD aided development of ibrutinib-loaded nanostructured lipid carriers aimed for lymphatic targeting: evaluation using chylomicron flow blocking approach. *Drug Deliv Transl Res*. 2020;10(5):1476–94. <https://doi.org/10.1007/s13346-020-00803-7>.
16. Shrivastava S, Gidwani B, Kaur CD. Development of mebendazole loaded nanostructured lipid carriers for lymphatic targeting: optimization, characterization, in-vitro and in-vivo evaluation. *Part Sci Technol*. 2021;39(3):380–90. <https://doi.org/10.1080/02726351.2020.1750515>.
17. Costa P, Sousa Lobo JM. Modeling and comparison of dissolution profiles. *Eur J Pharm Sci*. 2001;13(2):123–33. [https://doi.org/10.1016/S0928-0987\(01\)00095-1](https://doi.org/10.1016/S0928-0987(01)00095-1).
18. Faidi A, Lassoued MA, Becheikh MEH, Touati M, Stumbé JF, Farhat F. Application of sodium alginate extracted from a Tunisian brown algae *Padina pavonica* for essential oil encapsulation: microspheres preparation, characterization and in vitro release study. *Int J Biol Macromol*. 2019;136:386–94. <https://doi.org/10.1016/j.ijbiomac.2019.06.023>.
19. Patel N, Baldaniya M, Raval M, Sheth N. Formulation and development of in situ nasal gelling systems for quetiapine fumarate-loaded mucoadhesive microemulsion. *J Pharm Innov*. 2015;10(4):357–73.
20. Moghddam SMM, Ahad A, Aqil M, Imam SS, Sultana Y. Optimization of nanostructured lipid carriers for topical delivery of nimesulide using Box-Behnken design approach. *Artificial Cells, Nanomedicine, and Biotechnology*. 2017;45(3):617–24. <https://doi.org/10.3109/21691401.2016.1167699>.
21. Tapeinos C, Battaglini M, Ciofani G. Advances in the design of solid lipid nanoparticles and nanostructured lipid carriers for targeting brain diseases. *J Control Release*. 2017;264:306–32. <https://doi.org/10.1016/j.jconrel.2017.08.033>.
22. Pinto F, de Barros DPC, Reis C, Fonseca LP. Optimization of nanostructured lipid carriers loaded with retinoids by central composite design. *J Mol Liq*. 2019;293: 111468. <https://doi.org/10.1016/j.molliq.2019.111468>.
23. Hejri A, Khosravi A, Gharanjig K, Hejazi M. Optimisation of the formulation of β -carotene loaded nanostructured lipid carriers prepared by solvent diffusion method. *Food Chem*. 2013;141(1):117–23. <https://doi.org/10.1016/j.foodchem.2013.02.080>.
24. Zhang J, Fan Y, Smith E. Experimental design for the optimization of lipid nanoparticles. *J Pharm Sci*. 2009;98(5):1813–9. <https://doi.org/10.1002/jps.21549>.
25. Vitorino C, Carvalho FA, Almeida AJ, Sousa JJ, Pais AACC. The size of solid lipid nanoparticles: an interpretation from experimental design. *Colloids Surf, B*. 2011;84(1):117–30. <https://doi.org/10.1016/j.colsurfb.2010.12.024>.
26. Fathi HA, Allam A, ElSabahy M, Fetih G, El-Badry M. Nanostructured lipid carriers for improved oral delivery and prolonged antihyperlipidemic effect of simvastatin. *Colloids Surf, B*. 2018;162:236–45. <https://doi.org/10.1016/j.colsurfb.2017.11.064>.
27. Gaba B, Fazil M, Ali A, Baboota S, Sahni JK, Ali J. Nanostructured lipid (NLCs) carriers as a bioavailability enhancement tool for oral administration. *Drug Delivery*. 2015;22(6):691–700. <https://doi.org/10.3109/10717544.2014.898110>.
28. Tan SW, Billa N, Roberts CR, Burley JC. Surfactant effects on the physical characteristics of Amphotericin B-containing nanostructured lipid carriers. *Colloids Surf, A*. 2010;372(1):73–9. <https://doi.org/10.1016/j.colsurfa.2010.09.030>.
29. Gaumet M, Vargas A, Gurny R, Delie F. Nanoparticles for drug delivery: the need for precision in reporting particle size parameters. *Eur J Pharm Biopharm*. 2008;69(1):1–9. <https://doi.org/10.1016/j.ejpb.2007.08.001>.
30. Danaei M, Dehghankhold M, Ataei S, Hasanzadeh Davarani F, Javanmard R, Dokhani A, et al. Impact of particle size and polydispersity index on the clinical applications of lipidic nano-carrier systems. *Pharmaceutics*. 2018;10(2):57.
31. Chuacharoen T, Sabliov CM. Stability and controlled release of lutein loaded in zein nanoparticles with and without lecithin and pluronic F127 surfactants. *Colloids Surf, A*. 2016;503:11–8. <https://doi.org/10.1016/j.colsurfa.2016.04.038>.
32. Witayaudom P, Klinkesorn U. Effect of surfactant concentration and solidification temperature on the characteristics and stability of nanostructured lipid carrier (NLC) prepared from rambutan (*Nephelium lappaceum* L.) kernel fat. *J Colloid Interface Sci*. 2017;505:1082–92. <https://doi.org/10.1016/j.jcis.2017.07.008>.
33. Freitas C, Müller RH. Effect of light and temperature on zeta potential and physical stability in solid lipid nanoparticle (SLNTM) dispersions. *Int J Pharm*. 1998;168(2):221–9. [https://doi.org/10.1016/S0378-5173\(98\)00092-1](https://doi.org/10.1016/S0378-5173(98)00092-1).
34. Rydhag L, Wilton I. The function of phospholipids of soybean lecithin in emulsions. *J Am Oil Chem Soc*. 1981;58(8):830–7. <https://doi.org/10.1007/BF02665591>.
35. Wang G, Wang T. Oxidative stability of egg and soy lecithin as affected by transition metal ions and pH in emulsion. *J Agric Food Chem*. 2008;56(23):11424–31. <https://doi.org/10.1021/jf8022832>.
36. Han F, Li S, Yin R, Liu H, Xu L. Effect of surfactants on the formation and characterization of a new type of colloidal drug delivery system: nanostructured lipid carriers. *Colloids Surf, A*. 2008;315(1):210–6. <https://doi.org/10.1016/j.colsurfa.2007.08.005>.
37. Das S, Chaudhury A. Recent advances in lipid nanoparticle formulations with solid matrix for oral drug delivery. *AAPS PharmSciTech*. 2011;12(1):62–76. <https://doi.org/10.1208/s12249-010-9563-0>.
38. Iqbal MA, Md S, Sahni JK, Baboota S, Dang S, Ali J. Nanostructured lipid carriers system: recent advances in drug delivery. *J Drug Target*. 2012;20(10):813–30. <https://doi.org/10.3109/1061186X.2012.716845>.
39. Muchow M, Maincent P, Muller RH. Lipid nanoparticles with a solid matrix (SLN, NLC, LDC) for oral drug delivery. *Drug Dev Ind Pharm*. 2008;34(12):1394–405. <https://doi.org/10.1080/03639040802130061>.
40. Müller RH, Radtke M, Wissing SA. Nanostructured lipid matrices for improved microencapsulation of drugs. *Int J Pharm*. 2002;242(1):121–8. [https://doi.org/10.1016/S0378-5173\(02\)00180-1](https://doi.org/10.1016/S0378-5173(02)00180-1).
41. Katouzian I, Faridi Esfanjani A, Jafari SM, Akhavan S. Formulation and application of a new generation of lipid nano-carriers

- for the food bioactive ingredients. *Trends Food Sci Technol*. 2017;68:14–25. <https://doi.org/10.1016/j.tifs.2017.07.017>.
42. Shah B, Khunt D, Misra M, Padh H. Application of Box-Behnken design for optimization and development of quetiapine fumarate loaded chitosan nanoparticles for brain delivery via intranasal route*. *Int J Biol Macromol*. 2016;89:206–18. <https://doi.org/10.1016/j.ijbiomac.2016.04.076>.
 43. Gohel MC, Patel TM. Compatibility study of quetiapine fumarate with widely used sustained release excipients. *J Therm Anal Calorim*. 2013;111(3):2103–8. <https://doi.org/10.1007/s10973-012-2467-3>.
 44. Hernández Y, Lozano T, Morales-Cepeda AB, Navarro-Pardo F, Ángeles ME, Morales-Zamudio L, et al. Stearic acid as interface modifier and lubricant agent of the system: Polypropylene/calcium carbonate nanoparticles. *Polym Eng Sci*. 2019;59(s2):E279–85. <https://doi.org/10.1002/pen.25053>.
 45. Paliwal R, Rai S, Vaidya B, Khatri K, Goyal AK, Mishra N, et al. Effect of lipid core material on characteristics of solid lipid nanoparticles designed for oral lymphatic delivery. *Nanomed Technol Biol Med*. 2009;5(2):184–91. <https://doi.org/10.1016/j.nano.2008.08.003>.
 46. Das S, Ng WK, Tan RBH. Are nanostructured lipid carriers (NLCs) better than solid lipid nanoparticles (SLNs): development, characterizations and comparative evaluations of clotrimazole-loaded SLNs and NLCs? *Eur J Pharm Sci*. 2012;47(1):139–51. <https://doi.org/10.1016/j.ejps.2012.05.010>.
 47. Agarwal S, HariKumar SL, Negi P, Upadhyay N, Garg R. Quetiapine fumarate loaded nanostructured lipid carrier for enhancing oral bioavailability: design, development and pharmacokinetic assessment. *Curr Drug Deliv*. 2021;18(2):184–98. <https://doi.org/10.2174/1567201817999200728135119>.
 48. Narala A, Veerabrahma K. Preparation, characterization and evaluation of quetiapine fumarate solid lipid nanoparticles to improve the oral bioavailability. *J Pharm*. 2013;2013: 265741. <https://doi.org/10.1155/2013/265741>.
 49. Son GH, Lee BJ, Cho CW. Mechanisms of drug release from advanced drug formulations such as polymeric-based drug-delivery systems and lipid nanoparticles. *J Pharm Investig*. 2017;47(4):287–96. <https://doi.org/10.1007/s40005-017-0320-1>.
 50. Porter CJH, Pouton CW, Cuine JF, Charman WN. Enhancing intestinal drug solubilisation using lipid-based delivery systems. *Adv Drug Deliv Rev*. 2008;60(6):673–91. <https://doi.org/10.1016/j.addr.2007.10.014>.
 51. Porter CJH, Trevaskis NL, Charman WN. Lipids and lipid-based formulations: optimizing the oral delivery of lipophilic drugs. *Nat Rev Drug Discovery*. 2007;6(3):231–48. <https://doi.org/10.1038/nrd2197>.
 52. Zhuang CY, Li N, Wang M, Zhang XN, Pan WS, Peng JJ, et al. Preparation and characterization of vinpocetine loaded nanostructured lipid carriers (NLC) for improved oral bioavailability. *Int J Pharm*. 2010;394(1):179–85. <https://doi.org/10.1016/j.ijpharm.2010.05.005>.
 53. Li H, Zhao X, Ma Y, Zhai G, Li L, Lou H. Enhancement of gastrointestinal absorption of quercetin by solid lipid nanoparticles. *J Control Release*. 2009;133(3):238–44. <https://doi.org/10.1016/j.jconrel.2008.10.002>.
 54. Costa FO, Sousa JJS, Pais AACC, Formosinho SJ. Comparison of dissolution profiles of Ibuprofen pellets. *J Control Release*. 2003;89(2):199–212. [https://doi.org/10.1016/S0168-3659\(03\)00033-6](https://doi.org/10.1016/S0168-3659(03)00033-6).
 55. Öztürk AA, Aygül A, Şenel B. Influence of glyceryl behenate, tripalmitin and stearic acid on the properties of clarithromycin incorporated solid lipid nanoparticles (SLNs): formulation, characterization, antibacterial activity and cytotoxicity. *J Drug Delivery Sci Technol*. 2019;54: 101240. <https://doi.org/10.1016/j.jddst.2019.101240>.
 56. Rehman M, Ihsan A, Madni A, Bajwa SZ, Shi D, Webster TJ, et al. Solid lipid nanoparticles for thermoresponsive targeting: evidence from spectrophotometry, electrochemical, and cytotoxicity studies. *Int J Nanomedicine*. 2017;12:8325–36. <https://doi.org/10.2147/IJN.S147506>.
- Publisher's Note** Springer Nature remains neutral with regard to jurisdictional claims in published maps and institutional affiliations.